Heliyon

Received:
17 July 2018
Revised:
21 December 2018
Accepted:
22 February 2019

Cite as: Christina Schaub, Mischa Uebachs. Scaling of recovery rates influences T-type Ca^{2+} channel availability following IPSPs. Heliyon 5 (2019) e01278. doi: 10.1016/j.heliyon.2019.e01278

Scaling of recovery rates influences T-type Ca^{2+} channel availability following IPSPs

Christina Schaub [a,b], **Mischa Uebachs** [a,b,*]

[a] *Laboratory for Experimental Epileptology and Cognition Research, Department of Epileptology, Life & Brain Center, Sigmund Freud Str. 2, 53121, Bonn, Germany*

[b] *Department of Neurology, University of Bonn, Sigmund Freud Str. 2, 53121, Bonn, Germany*

[*] Corresponding author.

E-mail address: m.uebachs@uni-bonn.de (M. Uebachs).

Abstract

The excitability of neuronal membranes is crucially modulated by T-type Ca^{2+} channels (I_{CaT}) due to their low threshold of activation. I_{CaT} inactivates steeply at potentials close to the resting membrane potential. Therefore, the availability of I_{CaT} following changes in membrane potential depends on the time course of the onset of inactivation as well as on the time course of recovery from inactivation.

It was previously shown that the time course of recovery from inactivation depends on the duration of the conditioning pulse in cloned T-type Ca^{2+} channel subunits ($Ca_v3.1$-$Ca_v3.3$(Uebachs et al., 2006)). This provides a potential mechanism for an intrinsic form of short term plasticity. Here, we address the question, whether this mechanism results in altered availability of I_{CaT} following physiological changes in membrane potential. We found that the recovery of I_{CaT} during an IPSP depends on the duration of a preceding depolarized period.

Keyword: Biophysics

https://doi.org/10.1016/j.heliyon.2019.e01278

1. Introduction

T-type Ca^{2+} currents crucially determine neuronal excitability. They are located in the somatodendritic compartment of many types of neurons (Carbone and Lux, 1984; Talley et al., 1999) and have a low threshold of activation. This renders them capable of firing low-threshold Ca^{2+} spikes (Greene et al., 1986; Jahnsen and Llinás, 1984a, 1984b) and can switch the firing mode of cells from normal firing behaviour to burst firing (Kim et al., 2001; Su et al., 2002). On a network level, they are involved in the generation of intrinsic rhythms (Huguenard, 1996). Their role in neurological functions and diseases like pain perception and hyperalgesia (Ikeda et al., 2003; Kim et al., 2003), epilepsy (Su et al., 2002; Tsakiridou et al., 1995), mechanoreceptor function (Shin et al., 2003), to olfaction (Kawai and Miyachi, 2001), as well as the maintenance of sleep states (Anderson et al., 2005) was demonstrated by pharmacological and genetic inhibition.

Besides their low threshold of activation, T-type Ca^{2+} channels have a steep voltage dependent inactivation in the vicinity of the resting membrane potential (Uebachs et al., 2006). Therefore, the availability of T-type Ca^{2+} channels depends on slight changes in membrane potential. However, inactivation and recovery from inactivation are dynamic processes. Following membrane depolarization, onset of inactivation of T-type Ca^{2+} channels reaches steady-state within seconds. The time-course of recovery from inactivation was shown to be dependent of the duration of the previous depolarization (Uebachs et al., 2006). As a consequence, availability of T-type Ca^{2+} channels would not only reflect the actual membrane potential but integrate prior alterations. This was thought to provide a mechanism for intrinsic short-term plasticity.

However, the voltage steps examined in (Uebachs et al., 2006) were far more pronounced than membrane potential changes observed in physiological conditions. Since a large fraction of T-type Ca^{2+} channels is inactivated at resting membrane potential, hyperpolarization - as it occurs during inhibitory post synaptic potentials - is required to enable them to recover from inactivation, a process also termed de-inactivation.

In this study we address the question, if scaling of recovery rates occurs following slight changes of membrane potential and if this influences the de-inactivation of T-type Ca^{2+} channels during inhibitory potentials.

2. Materials and methods

2.1. Stably transfected HEK-293 cells

The generation of stable cell lines expressing human $Ca_v3.1$, $Ca_v3.2$ and $Ca_v3.3$ has been described previously. The following stably transfected HEK-293 cell lines

https://doi.org/10.1016/j.heliyon.2019.e01278

were used in this study: hα1G-Q39, containing the human α1G channel, $Ca_v3.1a$ (GenBank accession number AF190860, (Cribbs et al., 2000)); hh8-5, containing the Hh8 plasmid construct of human α1H, $Ca_v3.2a$ (GenBank accession number AF051946, (Cribbs et al., 1998)); and Lt9-8, containing the LT9 plasmid construct of α1I, $Ca_v3.3b$, (Gomora et al., 2002), GenBank accession number AF393329). Cells were maintained in DMEM media (4.5 g/l glucose, 584 mg/l L-glutamine) supplemented with 1 mg/mL of geneticin, 10% heat-inactivated foetal bovine serum, 100 units/mL penicillin and 100 μg/mL streptomycin.

2.2. Patch-clamp recording

Patch-clamp recordings were obtained from ~350 HEK cells expressing Ca_v3 Ca^{2+} channels. Patch pipettes with a resistance of 3−4 MΩ were fabricated from borosilicate glass capillaries and filled with an intracellular solution containing (in mM): Cs-methanesulfonate 87.5, $MgCl_2$ 5, $CaCl_2$ 0.5, tetraethylammonium 20, HEPES 10, bis-(o-aminophenoxy)-N,N,N‘,N‘-tetraacetic acid (BAPTA) 5, sucrose 16, adenosine-5’-triphosphate (Na_2^+-ATP) 10, guanosine-5’-triphosphate (GTP) 0.5 and glucose 10 (pH 7.2, 300 mosmol). BAPTA was used to avoid effects of intracellular Calcium to address the biophysical properties of the channels. Patch-clamp recordings from HEK cells were performed in a bath solution containing (in mM): sodium-methanesulfonate 125, KCl 3, $MgCl_2$ 1, $CaCl_2$ 5, 4-AP 4, tetraethylammonium 20, HEPES 10, glucose 10 (pH 7.4, 315 mosmol). Tight-seal whole-cell recordings were obtained at room temperature (21−24 °C) according to standard techniques (Sigworth et al., 1995). Membrane currents were recorded using a patch clamp amplifier (EPC9, HEKA Elektronik, Lambrecht/Pfalz, Germany) and collected on-line with the ’PULSE’ acquisition and analysis program (HEKA Elektronik, Lambrecht/Pfalz, Germany). Series resistance compensation was employed to improve the voltage-clamp control (>80%) so that the maximal residual voltage error did not exceed 1.5 mV (Sigworth et al., 1995). A liquid junction potential of 5 mV was measured between the intra- and extracellular solution and corrected on-line such that without correction, the voltages given in this paper would be 5 mV more positive. Holding potential was -70 mV.

2.3. Voltage protocols and data analysis

The onset of inactivation of T-type Ca^{2+} currents was described by holding the membrane potential to -60 mV for varying durations (t_{pre}) and a subsequent step to -25 mV (Fig. 1a). The peak current amplitude elicited (Fig. 1b) was normalized to the maximal amplitude elicited without a prepulse to −60 mV. The relation between the normalized peak amplitude and the prepulse duration was best fit by a biexponential equation of the form:

https://doi.org/10.1016/j.heliyon.2019.e01278

$$I(t_{pre}) = A_0 + A_1 * \exp(-t_{pre}/\tau_1) + A_2 * \exp(-t_{pre}/\tau_2) \quad (1)$$

where $I(t_{pre})$ is the current amplitude following a prepulse duration of t_{pre}, A_0 is a constant offset, and $\tau_1$and τ_2 the time constants of inactivation with the corresponding amplitudes A_1 and A_2, respectively.

Recovery from inactivation was examined with double pulse experiments (Fig. 2a). We addressed recovery of T-type Ca^{2+} channels following continuous step depolarizations to -60 mV of varying durations (t_{pre}:1−100 s). Recovery of T-type Ca^{2+} channels following these conditioning prepulses was examined by stepping the membrane potential back to −70 mV holding potential for a varying recovery interval (Δt, 40 ms to 20.5 seconds) and subsequently applying a brief (300 ms) test pulse to −25 mV. In all experiments, an equivalent normalization test pulse to −25 mV (300 ms) was applied before each double pulse. Normalization of the recovery data was then carried out with the amplitude of the current elicited during this normalization test pulse.

We were concerned that rundown of Ca^{2+} current amplitudes might contaminate our results. Therefore, we excluded all experiments in which the Ca^{2+} current amplitudes elicited by the normalization test pulse (see description of double-pulse protocols above) were reduced by more than 20% over 1.5 hours of recording from further analysis. We also excluded experiments in which the input resistance measured in recording solution was <1GΩ, or cells in which a transient change in passive membrane properties was observed. The time constants of recovery τ_{fast} and τ_{slow} were extracted by fitting with a biexponential equation of the form:

$$I(t) = A_0 + A_{fast} * \left(1 - \exp\left(-\Delta t/\tau_{fast}\right)\right) + A_{slow} * (1 - \exp(-\Delta t/\tau_{slow})) \quad (2)$$

The amplitude proportion of the fast (A_{fast}) and the slow (A_{slow}) component were linked in a simultaneous fit and thereby identical for all prepule durations.

In some cases, fitting was carried out with a monoexponential equation of an identical form when a biexponential equation resulted in equal time-constants or a corresponding amplitude proportion <10%.

The recovery from inactivation during physiological hyperpolarizations was examined by application of an inactivating depolarization, a subsequently applied mock IPSP that mimics a recorded IPSP, and a test-pulse to -25 mV (400 ms) to assess the fraction of available T-type Ca^{2+} channels (Fig. 3a).

Data was fit using Origin (OriginLab Corp, Northhampton). All results are shown as the mean ± S.E.M. Statistical comparison was carried out with a two-tailed Student's t-test.

https://doi.org/10.1016/j.heliyon.2019.e01278

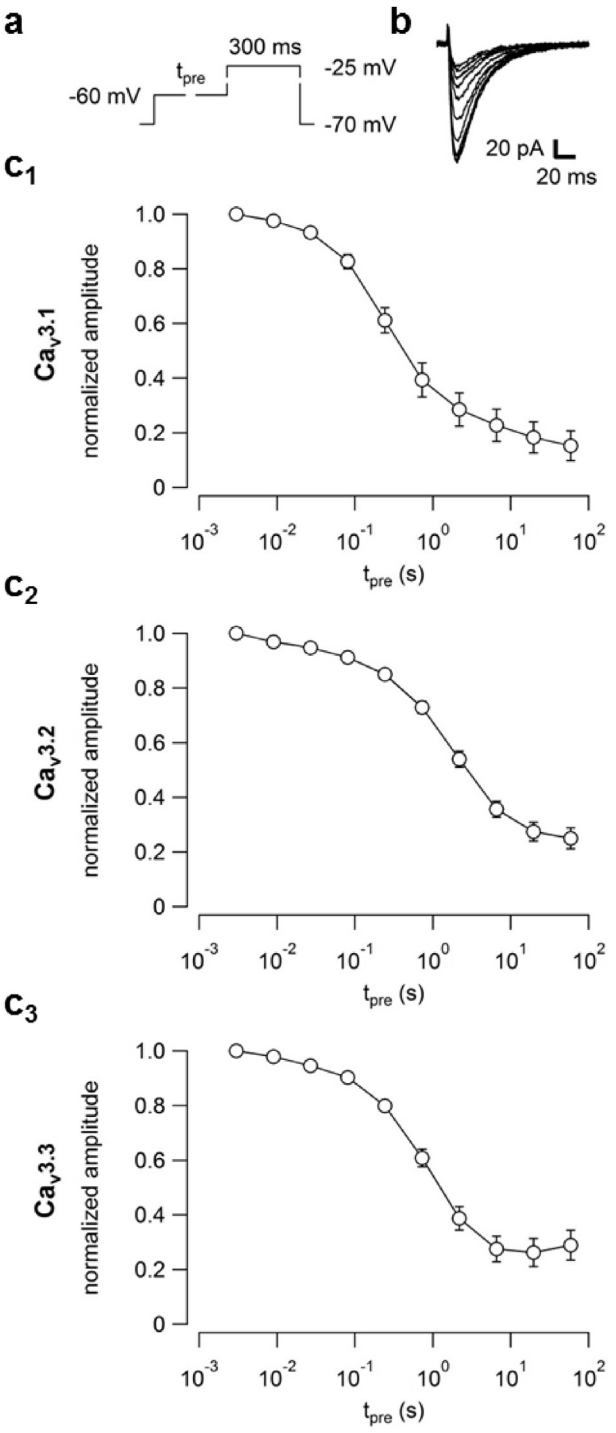

Fig. 1. The onset of inactivation is similar for all three Ca_V3 subtypes. Onset of inactivation was examined using standard protocols (panel a, representative current traces in panel b). Slight depolarizations from -70 to -60 mV were sufficient to inactivate most T-type Ca^{2+} channels (remaining fraction given as $A_{steadystate}$ in Table 1). The time-course was similar for all three subtypes (panel c_1-c_3) and best described by a biexponential function (time constants τ_{fast} and τ_{slow} and the relative proportion of τ_{fast} (A_{fast}) are given in Table 1, $n \geq 7$).

https://doi.org/10.1016/j.heliyon.2019.e01278

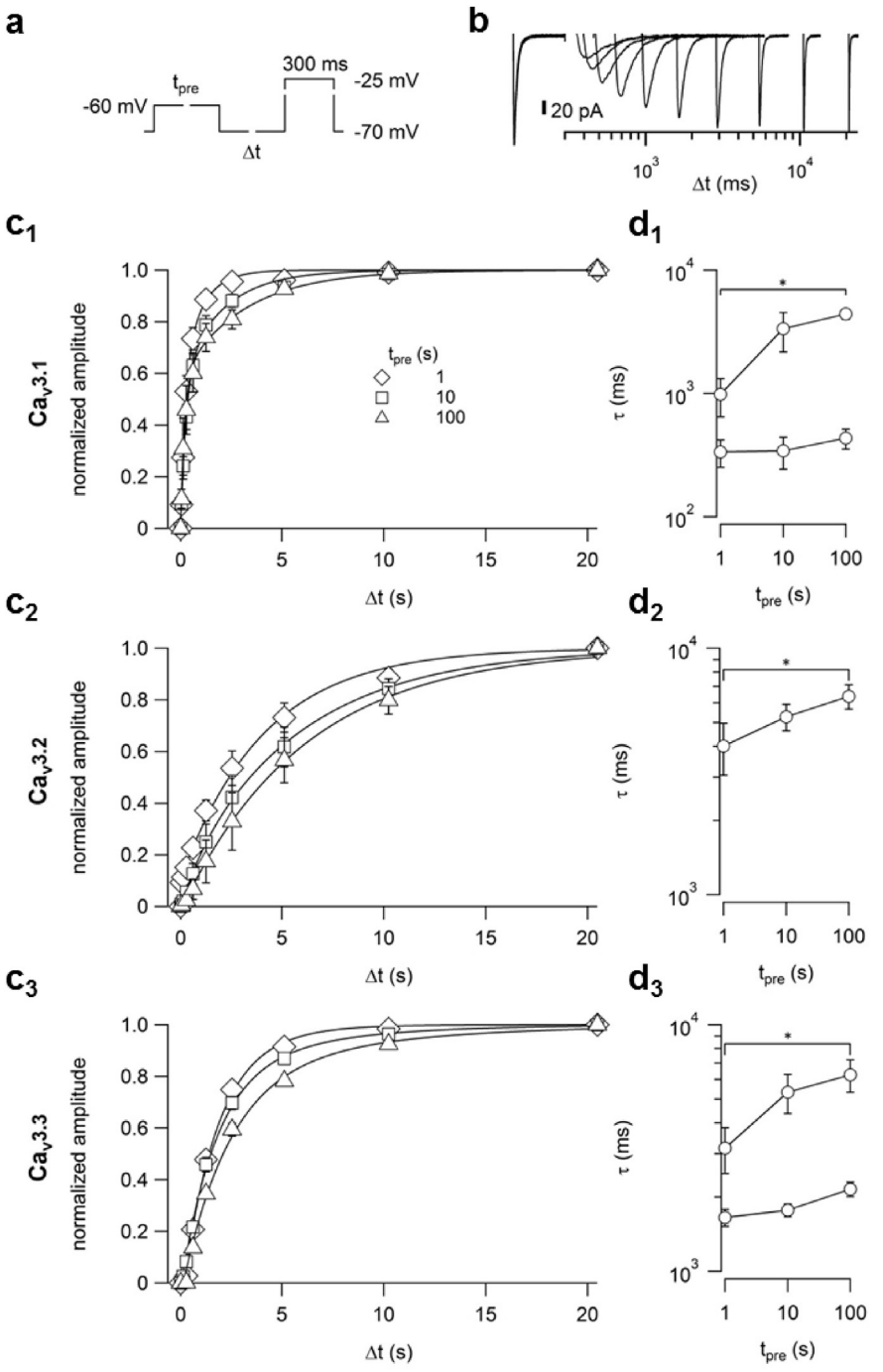

Fig. 2. The recovery rates depend on the duration of the inactivating depolarization. T-type Ca^{2+} channels were inactivated by a voltage step from -70 to -60 mV of varying duration (t_{pre}: 1−100s). Following subsequent steps to -70 mV of increasing duration (40 ms−20 s) to allow channels to recover from inactivation, channel availability was assessed with a test pulse to -25mV (panel a, representative current traces in panel b). Current amplitude was normalized to the maximum current elicited by a test pulse not preceded by an inactivating stimulus and depicted versus the recovery interval (panel c_1-c_3, circles, squares and triangles correspond to prepulse durations of 1, 10 and 100s, respectively, n = 5−8). Datasets for all prepulse durations were fit simultaneously with a biexponential function (for $Ca_v3.2$

https://doi.org/10.1016/j.heliyon.2019.e01278

3. Results

3.1. Onset of inactivation

First we examined the time course of the onset of inactivation of cloned Ca^{2+} T-type channels ($Ca_v3.1$ - $Ca_v3.3$) expressed in HEK293 cells. A test-pulse to -25 mV (300 ms) was applied following a preceding depolarization of varying duration (3 ms−59 s) to -60 mV from a holding potential of -70 mV (Fig. 1a). The peak amplitude of the elicited current (Fig. 1b) was normalized to the peak amplitude of the current elicited by a test-pulse without previous depolarization. The relative amplitude was averaged for all recorded cells and depicted versus the duration of the preceding depolarization for all three T-type Ca^{2+} channel subtypes examined (Fig. 1c_1-c_3 for $Ca_v3.1$-$Ca_v3.3$ respectively). This reveals that a relevant fraction of channels inactivates within a time period $<$ 1s and a steady state inactivation of $\sim$80% of the channels available at the holding potential (-70 mV) is reached within 10−100 s in all three T-type Ca^{2+} channel subtypes (see Table 1).

3.2. Recovery from inactivation

Previous studies (Uebachs et al., 2006) have shown that the time-course of recovery from inactivation depends on the duration of the depolarizing voltage step that induces the inactivation. In a similar set of experiments we addressed the question, if this scaling of recovery rates also occurs following small changes in membrane potential as observed during physiological processes. We applied a small depolarizing step to -60 mV (from a holding potential of -70 mV) of varying duration (t_{pre}: 1−100 s) to inactivate the T-type Ca^{2+} channels (relative current amplitude interpolated according to the recordings in Fig. 1 are given in Table 2). Subsequently we enabled the channels to recover from inactivation during an increasing period (Δt: 80 ms to 20 s) at -70 mV. Finally a test-pulse to -25 mV was applied (Fig. 2a). The amplitude of the elicited current increased with prolonged recovery intervals (Fig. 2b). The fraction of available T-type Ca^{2+} channels was quantified relative to the amount of channels available at holding potential (-70 mV) obtained by a test-pulse without preceding depolarization, averaged for all recorded cells and depicted versus the recovery interval (Δt) for all three T-type Ca^{2+} channel subtypes (Fig. 2c_1-c_3 for $Ca_v3.1$-$Ca_v3.3$ respectively). Consistent with existing data (Uebachs et al., 2006), the time-course of recovery from inactivation is dependent on the duration of the inactivating depolarization even in the more physiological range of membrane potential changes used in this study. The time course of recovery

monoexponential, see methods section). The amplitude proportion of fast and slow recovering fractions were linked (Fits depicted as solid lines superimposed on datapoints in panels c_1-c_3). Prolonged prepulse durations resulted in increased time constants in all three subtypes (panel d_1-d_3, significant when comparing 1s to 100s, indicated by asterisks).

https://doi.org/10.1016/j.heliyon.2019.e01278

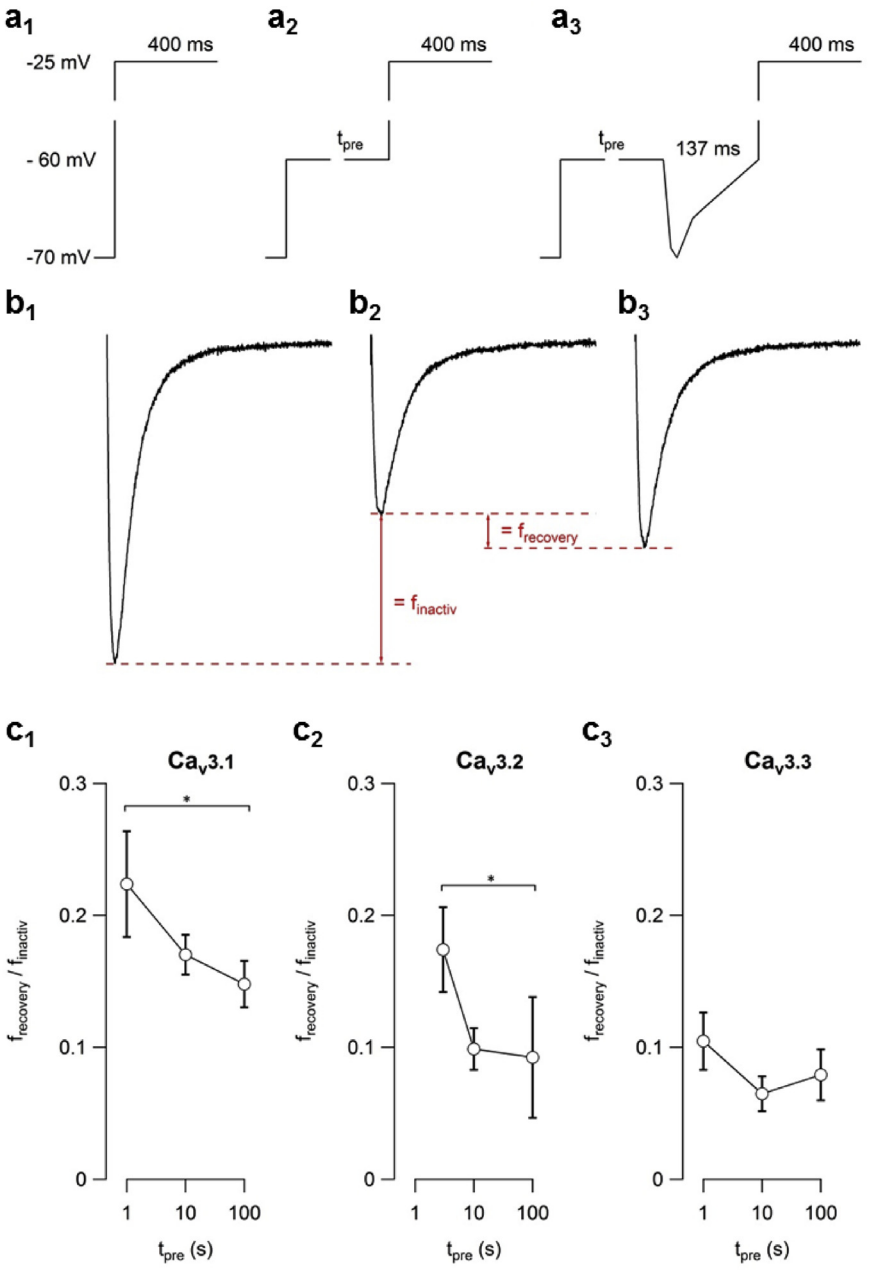

Fig. 3. Slowing of recovery reduces T-type Ca^{2+} channel availability following IPSPs. T-type Ca^{2+} channels were activated with a depolarizing voltage step to -25mV (panel a_1, representative current trace in a_1). Subsequently, channel availability was measured following a depolarizing step (1−100 s) to -60mV (panel a_2) to determine the inactivated fraction (panel b_2). Finally, the same inactivating voltage step was applied followed by a mock IPSP and the test-pulse to -25mV (panel a_3). The recovering fraction was defined as the increase of the current amplitude compared to panel b_2 (see panel b_3). This fraction was normalized to the inactivated fraction and plotted versus the duration of the inactivating stimulus (panel c_1-c_3, $n \leq 7$). Prolonged depolarization slows down the recovery (see Fig. 2) resulting in a smaller fraction recovering during the IPSP for $Ca_v3.1$ and $Ca_v3.2$ channels (panel $c_1$and c_2, significant when comparing 1s to 100s, indicated by asterisks). For $Ca_v3.3$ the recovering fraction was independent of the prepulse duration (panel c_3).

https://doi.org/10.1016/j.heliyon.2019.e01278

Table 1. Biexponential fit of the onset of inactivation of the three T-type Ca^{2+} channel isoforms.

	$Ca_V3.1$	$Ca_V3.2$	$Ca_V3.3$
$A_{steadystate}$	0.16 ± 0.05	0.24 ± 0.03	0.27 ± 0.05
τ_{fast} (s)	0.64 ± 0.06	0.25 ± 0.03	0.28 ± 0.08
A_{fast} (%)	3.9 ± 0.5	9.5 ± 2.2	12.6 ± 4.5
τ_{slow} (s)	0.19 ± 0.01	0.50 ± 0.05	0.45 ± 0.06

was fit with a biexponential equation (see Methods section) for each individual cell. The slowing of recovery of $Ca_v3.1$ and $Ca_v3.3$ channels apparent in Fig. 2c_1 and c_3 was mainly represented by an increase of the slow time-constant as depicted in Fig. 2d_1 and d_3. In the case of $Ca_v3.2$ the amplitude proportion of one time constant turned out to be negligible and a monoexponential equation obtained a proper fit of the data with an increasing time-constant with prolonged inactivating stimulus.

Taken together the data confirm that even slight changes in membrane potential induce scaled dynamics of recovery from inactivation.

3.3. Recovery during IPSPs

Physiological changes of membrane potential are frequently caused by post synaptic potentials. Particularly for the T-type Ca^{2+} channel which is located mainly on the dendrites modulating the neuronal response to synaptic input, hyperpolarization as a consequence of inhibitory GABAergic input is essential to remove inactivation. To address the question, whether scaling of recovery rates influences the availability of T-type Ca^{2+} channels following inhibitory postsynaptic potentials (IPSP) we first assessed the maximal fraction of T-type Ca^{2+} channels available (representative current trace in Fig. 3b_1). Therefore, we applied a test-pulse to -25 mV (400 ms) from a holding potential of -70 mV (Fig. 3a_1). Then we preceded the test-pulse by a depolarization of varying duration analog to the experiments described before (t_{pre}: 1−100 s, Fig. 3a_2) to inactivate T-type Ca^{2+} channels (Fig. 3b_2, $f_{inactiv}$). Finally, the depolarizing voltage step was followed by a mock IPSP to enable T-type Ca^{2+} channels to recover from inactivation and a subsequent test-pulse to asses the fraction of channels available (Fig. 3a_3). The fraction of T-type Ca^{2+} channels that recover during the mock IPSP ($f_{recovery}$, Fig. 3b_3) relative to the fraction of inactivated channels ($f_{inactiv}$, Fig. 3b_2) is obtained for each individual cell, averaged and depicted versus the duration of the inactivating stimulus (Fig. 3$c_{1\text{-}3}$). In all T-type Ca^{2+} channel subtypes ~10−25% of the channels that inactivated during the depolarization recovered during the mock IPSP. For $Ca_v3.1$ and $Ca_v3.2$ the magnitude of this fraction was reduced with more prolonged depolarizations (Fig. 3c_1 and c_3, asterisks indicate p-value<0.05). This is likely due to the slower recovery from inactivation following more prolonged depolarizations. For $Ca_v3.3$ no significant

https://doi.org/10.1016/j.heliyon.2019.e01278

Table 2. Relative amplitude of I_{Ca} following the prepulses applied in Figs. 2 and 3.

	$Ca_V3.1$	$Ca_V3.2$	$Ca_V3.3$
1s	0.38	0.68	0.54
10 s	0.20	0.32	0.29
100 s	0.17	0.24	0.27

changes in the recovery of T-type Ca^{2+} channels during the mock IPSP could be observed (Fig. $3c_3$).

Our data suggest that the scaling of recovery results in an altered availability of T-type Ca^{2+} channels following IPSPs and suggest that this channel intrinsic property has implications for modulating the availability of T-type channels during physiological activity.

4. Discussion

The integration of incoming inhibitory and excitatory inputs to an action potential output is a key feature of neurons in the context of a network. This process is determined by the properties of excitatory and inhibitory synapses, but is also importantly determined by intrinsic neuronal excitability (Beck and Yaari, 2008). In particular, the expression of voltage-gated ion channels is a key determinant both of dendritic integration and somatic action potential output generation. The presence of voltage-gated channels confer complex electrical properties on somatodendritic neuronal compartments, due to the time- and voltage-dependent gating of these conductances. In this context, slower voltage-dependent inactivation processes have been recognized as important in modulating the availability of many channels, amongst them sodium and calcium channels. For both of the ion channel types, scaling of recovery rates can constitute an intriguing mechanism for complex activity-dependent modulation of channel availability, and has been discussed as an intrinsic mechanism of short term plasticity (Uebachs et al., 2006). However, many of these studies have utilized strong depolarizations to induce slow inactivation, which are unlikely to occur in a physiological context. In this study, we demonstrate that even slight membrane potential changes within a physiological range (-70 to -60 mV) are sufficient to inactivate a relevant fraction of T-type Ca^{2+} channels ($\sim$80%, Fig. 1) on a timescale of seconds. Consistent with previous findings the recovery from this inactivated state depends on the duration (1−100 s) of the preceding depolarizing step. (Fig. 2). Such depolarizations likely occur under physiological circumstances in-vivo. In many cells up- and down states can be observed, in which the membrane potential switches in a bistable manner between more hyperpolarized and more depolarized levels.

https://doi.org/10.1016/j.heliyon.2019.e01278

These depolarizations are within the range that would induce substantial inactivation of T-type Ca^{2+} channels (Fig. 1).

Since recent work indicates that the inactivation behavior of T-type Ca^{2+} channels is modulated by intracellular Ca^{2+} levels (Cazade et al., 2017; Chemin et al., 2017) the demonstrated effects could be due to this secondary mechanism instead of the intrinsic electrophysiological properties. To minimize this effect we applied a high concentration of intracellular Ca^{2+} buffer (BAPTA).

The availability of T-type channels in turn controls burst firing and low-threshold Ca^{2+} spike generation (Greene et al., 1986; Jahnsen and Llinás, 1984b). In different brain regions, such as the cerebellum, thalamus and brain stem, a modulation of T-type channel availability was shown to contribute to rhythmogenesis (Huguenard, 1996). In addition, an important role of T-type Ca^{2+} channels has been demonstrated for sensory sytems (Ikeda et al., 2003; Kim et al., 2003), mechanoreceptor function (Shin et al., 2003), olfaction (Kawai and Miyachi, 2001) and the maintainance of sleep states (Anderson et al., 2005).

In many neurons expressing T-type Ca^{2+} channels, they are located in dendrites (Talley et al., 1999) and modulate the propagation of postsynaptic potentials from the distant dendrites to the soma (Christie et al., 1995; Magee et al., 1995; Magee and Johnston, 1995). In these compartments, a scaled recovery behavior during physiological hyperpolarizations - dependent on the duration of preceding depolarizations − would affect temporal integration of incoming excitatory and inhibitory input. When applying mock IPSPs following a prolonged depolarized period to mimic this physiological process a relevant fraction of the inactivated channels recovered during this mock IPSP. In fact, this fraction was smaller with increasing duration of the preceding depolarization (Fig. 3). This suggests that scaling of recovery rates can contribute to the modulation of postsynaptic excitability, making it dependent on prior alterations of the membrane potential. However, the behavior of the three isoforms is quite divers: In our findings only $Ca_V3.1$ and 3.1 display a de-inactivation dependent on the duration of the preceding depolarization. Interestingly, these two isoforms require more pronounced hyperpolarization to de-inactivate. In contrast, $Ca_V3.2$ has the slowest time-scale of recovery from inactivation (summarized in (Cain and Snutch, 2010), see also Fig. 2c_2 and d_2).

Thus, this biophysical property of T-type Ca^{2+} channels may provide an intrinsic mechanism of short term plasticity and temporal integration of synaptic inputs, an could be modulated by expression patterns of the Ca_V isoforms. However, the relevance for different neuronal and sensory systems was not addressed in this study and remains issue for further investigation.

https://doi.org/10.1016/j.heliyon.2019.e01278

Declarations

Author contribution statement

Mischa Uebachs: Conceived and designed the experiments; Performed the experiments; Analyzed and interpreted the data; Contributed reagents, materials, analysis tools or data; Wrote the paper.

Christina Schaub: Performed the experiments; Analyzed and interpreted the data; Contributed reagents, materials, analysis tools or data; Wrote the paper.

Funding statement

This research did not receive any specific grant from funding agencies in the public, commercial, or not-for-profit sectors.

Competing interest statement

The authors declare no conflict of interest.

Additional information

No additional information is available for this paper.

Acknowledgements

We thank Edward Perze-Reyes for providing the HEK293 cell lines used in this study.

References

Anderson, M.P., Mochizuki, T., Xie, J., Fischler, W., Manger, J.P., Talley, E.M., Scammell, T.E., Tonegawa, S., 2005. Thalamic Cav3.1 T-type Ca2+ channel plays a crucial role in stabilizing sleep. Proc. Natl. Acad. Sci. U. S. A. 102, 1743−1748.

Beck, H., Yaari, Y., 2008. Plasticity of intrinsic neuronal properties in CNS disorders. Nat. Rev. Neurosci. 9, 357−369.

Cain, S.M., Snutch, T.P., 2010. Contributions of T-type calcium channel isoforms to neuronal firing. Channels Austin. Tex. 4, 475−482.

Carbone, E., Lux, H.D., 1984. A low voltage-activated, fully inactivating Ca channel in vertebrate sensory neurones. Nature 310, 501−502.

Cazade, M., Bidaud, I., Lory, P., Chemin, J., 2017. Activity-dependent regulation of T-type calcium channels by submembrane calcium ions. eLife 6.

https://doi.org/10.1016/j.heliyon.2019.e01278

Chemin, J., Taiakina, V., Monteil, A., Piazza, M., Guan, W., Stephens, R.F., Kitmitto, A., Pang, Z.P., Dolphin, A.C., Perez-Reyes, E., Dieckmann, T., Guillemette, J.G., Spafford, J.D., 2017. Calmodulin regulates Cav3 T-type channels at their gating brake. J. Biol. Chem. 292, 20010–20031.

Christie, B.R., Eliot, L.S., Ito, K., Miyakawa, H., Johnston, D., 1995. Different Ca2+ channels in soma and dendrites of hippocampal pyramidal neurons mediate spike-induced Ca2+ influx. J. Neurophysiol. 73, 2553–2557.

Cribbs, L.L., Gomora, J.C., Daud, A.N., Lee, J.H., Perez-Reyes, E., 2000. Molecular cloning and functional expression of Ca(v)3.1c, a T-type calcium channel from human brain. FEBS Lett. 466, 54–58.

Cribbs, L.L., Lee, J.H., Yang, J., Satin, J., Zhang, Y., Daud, A., Barclay, J., Williamson, M.P., Fox, M., Rees, M., Perez-Reyes, E., 1998. Cloning and characterization of alpha1H from human heart, a member of the T-type Ca2+ channel gene family. Circ. Res. 83, 103–109.

Gomora, J.C., Murbartián, J., Arias, J.M., Lee, J.-H., Perez-Reyes, E., 2002. Cloning and expression of the human T-type channel Ca(v)3.3: insights into prepulse facilitation. Biophys. J. 83, 229–241.

Greene, R.W., Haas, H.L., McCarley, R.W., 1986. A low threshold calcium spike mediates firing pattern alterations in pontine reticular neurons. Science 234, 738–740.

Huguenard, J.R., 1996. Low-threshold calcium currents in central nervous system neurons. Annu. Rev. Physiol. 58, 329–348.

Ikeda, H., Heinke, B., Ruscheweyh, R., Sandkühler, J., 2003. Synaptic plasticity in spinal lamina I projection neurons that mediate hyperalgesia. Science 299, 1237–1240.

Jahnsen, H., Llinás, R., 1984a. Electrophysiological properties of Guinea-pig thalamic neurones: an in vitro study. J. Physiol. 349, 205–226.

Jahnsen, H., Llinás, R., 1984b. Ionic basis for the electro-responsiveness and oscillatory properties of Guinea-pig thalamic neurones in vitro. J. Physiol. 349, 227–247.

Kawai, F., Miyachi, E., 2001. Enhancement by T-type Ca2+ currents of odor sensitivity in olfactory receptor cells. J. Neurosci. Off. J. Soc. Neurosci. 21, RC144.

Kim, D., Park, D., Choi, S., Lee, S., Sun, M., Kim, C., Shin, H.-S., 2003. Thalamic control of visceral nociception mediated by T-type Ca2+ channels. Science 302, 117–119.

https://doi.org/10.1016/j.heliyon.2019.e01278

Kim, D., Song, I., Keum, S., Lee, T., Jeong, M.J., Kim, S.S., McEnery, M.W., Shin, H.S., 2001. Lack of the burst firing of thalamocortical relay neurons and resistance to absence seizures in mice lacking alpha(1G) T-type Ca(2+) channels. Neuron 31, 35–45.

Magee, J.C., Christofi, G., Miyakawa, H., Christie, B., Lasser-Ross, N., Johnston, D., 1995. Subthreshold synaptic activation of voltage-gated Ca2+ channels mediates a localized Ca2+ influx into the dendrites of hippocampal pyramidal neurons. J. Neurophysiol. 74, 1335–1342.

Magee, J.C., Johnston, D., 1995. Synaptic activation of voltage-gated channels in the dendrites of hippocampal pyramidal neurons. Science 268, 301–304.

Shin, J.-B., Martinez-Salgado, C., Heppenstall, P.A., Lewin, G.R., 2003. A T-type calcium channel required for normal function of a mammalian mechanoreceptor. Nat. Neurosci. 6, 724–730.

Sigworth, F.J., Affolter, H., Neher, E., 1995. Design of the EPC-9, a computer-controlled patch-clamp amplifier. 2. Software. J. Neurosci. Methods 56, 203–215.

Su, H., Sochivko, D., Becker, A., Chen, J., Jiang, Y., Yaari, Y., Beck, H., 2002. Upregulation of a T-type Ca2+ channel causes a long-lasting modification of neuronal firing mode after status epilepticus. J. Neurosci. Off. J. Soc. Neurosci. 22, 3645–3655.

Talley, E.M., Cribbs, L.L., Lee, J.H., Daud, A., Perez-Reyes, E., Bayliss, D.A., 1999. Differential distribution of three members of a gene family encoding low voltage-activated (T-type) calcium channels. J. Neurosci. Off. J. Soc. Neurosci. 19, 1895–1911.

Tsakiridou, E., Bertollini, L., de Curtis, M., Avanzini, G., Pape, H.C., 1995. Selective increase in T-type calcium conductance of reticular thalamic neurons in a rat model of absence epilepsy. J. Neurosci. Off. J. Soc. Neurosci. 15, 3110–3117.

Uebachs, M., Schaub, C., Perez-Reyes, E., Beck, H., 2006. T-type Ca2+ channels encode prior neuronal activity as modulated recovery rates. J. Physiol. 571, 519–536.

https://doi.org/10.1016/j.heliyon.2019.e01278